12

High-Frequency Fields: Magnetic Levitation and Induction Heating

> Electricity is of two kinds, positive and negative. The difference is, I presume, that one comes a little more expensive, but is more durable; the other is a cheaper thing, but the moths get in.
>
> *Stephen Leacock*

A high-frequency induction coil can be used to heat, levitate and stir liquid metal. This has given rise to a number of metallurgical processes, some old (such as induction furnaces) and some new. In this chapter, we shall discuss five.

(i) *Induction furnaces.* These have remained virtually unchanged for the best part of a century, yet we are still unable to calculate reliably the stirring velocity within a furnace!

(ii) *Cold crucible melting.* This is an ingenious process which combines the functions of an induction melter and a continuous caster, all in one device.

(iii) *Levitation melting.* This is now routinely used in the laboratory to melt small specimens of highly reactive metals. Unfortunately, if the levitated drop becomes too large, it tends to drip.

(iv) *The electromagnetic valve.* This provides a non-contact means of modulating and shaping a liquid-metal jet. It is a sort of levitation melter in which the metal is allowed to leak out of the bottom.

(v) *Electromagnetic casting.* Some aluminium producers have replaced the casting mould in a continuous caster by a high-frequency induction coil. Thus, the melt pool is supported by magnetic pressure rather than by mechanical means. It is extraordinary that large ingots, which may be a metre wide and ten metres long, can be formed by pouring the liquid metal into free space and soaking it with water jets!

These industrial processes are described in Section 3 of this chapter. First, however, there is some work to do. We need to develop expressions for the levitation force per unit area (magnetic pressure), the heating rate per

unit volume, and the stirring force (the rotational part of $\mathbf{J} \times \mathbf{B}$) induced by a high-frequency magnetic field.

12.1 The Skin Effect

We are concerned here with the ability of high-frequency magnetic fields to heat, levitate and stir liquids. All of these processes are controlled by the so-called *skin effect*: the ability of a conducting medium, solid or liquid, to exclude high-frequency fields. In this section, we describe (in words) the physical origin of this phenomenon. In Section 2, we will quantify the process.

The skin effect is most readily understood in the context of solid, rather than fluid, conductors, and so we start with solids. We have already seen that a magnetic field diffuses through a solid conductor according to

$$\frac{\partial \mathbf{B}}{\partial t} = \lambda \nabla^2 \mathbf{B} \tag{12.1}$$

We cannot suddenly *impose* a magnetic field throughout a conductor. All we can do is apply a field at the boundaries and then let it diffuse inward. In fact, we saw in Chapter 4 that a magnetic field diffuses inwards by a distance of under $(2\lambda t)^{1/2}$ in a time t. There is an analogy here with heat. Heat (temperature) diffuses through a thermally conducting medium according to

$$\frac{\partial T}{\partial t} = \alpha \nabla^2 T \tag{12.2}$$

If the surface temperature of a body is suddenly raised by an amount ΔT, then that temperature difference will diffuse inward into the conducting medium, travelling a distance of order $(2\alpha t)^{1/2}$ in a time t.

Let us stay with the thermal analogy as we consider oscillating, rather than steady, boundary conditions. Suppose that the temperature at the surface of some thermally conducting medium oscillates rapidly according to $T = T_0 + \Delta T \sin(\omega t)$, where T_0 is the initial bulk temperature of the medium. Heat is periodically injected into, and extracted from, the conductor. As successive waves of positive and negative temperature difference diffuse inward from the boundary, there is a tendency for them to overlap and cancel. In the limit of a high angular frequency, ω, the temperature fluctuations are felt only in a thin region adjacent to the surface, of thickness $\delta \sim (2\alpha/\omega)^{1/2}$ (Figure 12.1). (This is readily confirmed by looking for oscillatory solutions of (12.2).) What is true of

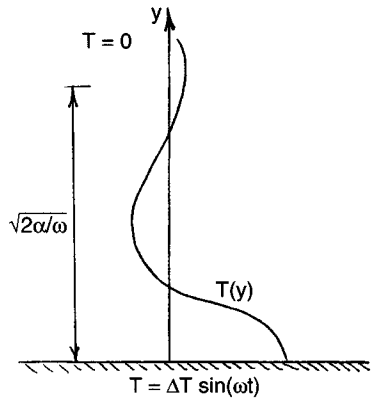

Figure 12.1 Thermal oscillations imposed at a boundary are restricted to thin boundary layers adjacent to that boundary.

T is also true of **B**. If an oscillating magnetic field is applied parallel to the surface of an electrically conducting medium, the field will penetrate only a finite distance, of order $(2\lambda/\omega)^{1/2}$, into the medium. This is illustrated in Figure 12.2.

Now if the magnetic field is excluded from the interior of the medium then there must be currents induced in the surface of the conductor whose direction is, in some average sense, opposite to that of the external currents which generated the field. That is to say, the magnetic field in the interior of the conducting medium is the superposition of two fields: one associated with the external currents and one associated with the induced currents, each calculated in accordance with the Biot–Savart law. If the combined field is to be zero in the interior then the external and induced currents must, in some average sense, oppose each other.

In general, then, a high-frequency magnetic field induces currents in the surface of a conductor whose distribution is such as to shield the interior of the conductor from the imposed field. These currents are restricted to a thin surface layer of thickness $\delta \sim (2\lambda/\omega)^{1/2}$, called the *skin depth*. In fact, we take as our working definition of the term 'high frequency' that δ must be much less than any relevant geometric length scale, say the characteristic size of the body. Now the fact that a magnetic field is shielded from the interior of a conductor is not, in itself, particularly important in metallurgical MHD. However, the existence of a thin surface layer of induced current is useful. Opposite currents repel each other, and so the conductor shown in Figure 12.2 will experience a sideways repulsion

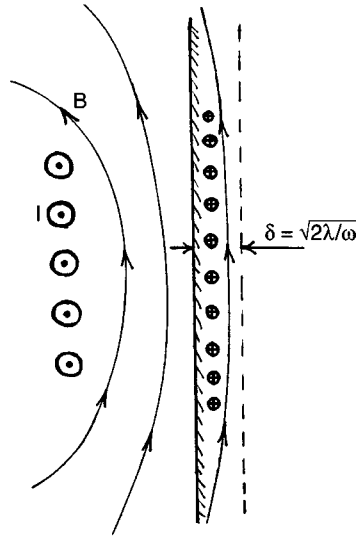

Figure 12.2 A high-frequency magnetic field is shielded from the interior of a conductor by the formation of surface currents which are restricted to a thin layer of thickness $(2\lambda/\omega)^{1/2}$.

force. Moreover, the induced currents will heat the conductor. It is the ability of high-frequency conductors to repel and heat conducting material, liquid or solid, which is the key to many industrial processes.

12.2 Magnetic Pressure, Induction Heating and High-Frequency Stirring

Let us now quantify the arguments of the previous section. We shall derive expressions for:

(i) the levitation force;
(ii) the surface heating rate;
(iii) the stirring force (the rotational part of $\mathbf{J} \times \mathbf{B}$).

Suppose that we have a magnetic field $\mathbf{B} = B_0 \cos(\omega t)\hat{\mathbf{e}}_z$ applied at the surface of a conducting fluid, as shown in Figure 12.3. In the first instance we shall take B_0 to be uniform. Let us assume that the velocity of the fluid is everywhere much less than ωl, where l is the smallest characteristic length scale of the problem. (This is almost always true in practice.) Then, for the purposes of calculating $\mathbf{B}$, we may treat the fluid as a

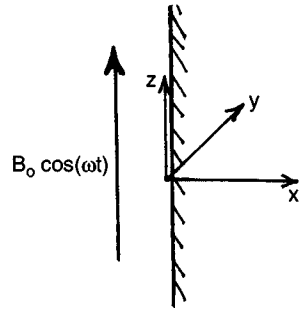

Figure 12.3 A simple model problem.

stationary, solid conductor. The governing equation for **B** simplifies to (12.1), which has the simple solution

$$\mathbf{B} = B_0 \exp(-x/\delta)\cos(\omega t - x/\delta)\hat{\mathbf{e}}_z, \qquad \delta = (2\lambda/\omega)^{1/2}$$

As expected, **B** is confined to a thin layer of thickness $\sim \delta$. The induced current is given by Ampère's law which, for this geometry, simplifies to

$$\mathbf{J} = -\frac{1}{\mu}\frac{\partial B_z}{\partial x}\hat{\mathbf{e}}_y \tag{12.3}$$

Substituting for B_z we find

$$J_y = (B_0/\mu\delta)\exp(-x/\delta)[\cos(\omega t - x/\delta) - \sin(\omega t - x/\delta)] \tag{12.4}$$

The Lorentz force within the skin depth can now be calculated:

$$\mathbf{J} \times \mathbf{B} = J_y B_z \hat{\mathbf{e}}_x = -\frac{\partial}{\partial x}\left[\frac{B_z^2}{2\mu}\right]\hat{\mathbf{e}}_x$$

This contains both a mean and an oscillatory component. However, we are interested only in the time-averaged value of the Lorentz force, since the finite inertia of the fluid means that a high-frequency, oscillatory force induces very little motion in the fluid. The time-averaged force is

$$\overline{\mathbf{J} \times \mathbf{B}} = -\frac{\partial}{\partial x}\left[\frac{B_0^2}{4\mu}\exp(-2x/\delta)\right]\hat{\mathbf{e}}_x \tag{12.5}$$

If we integrate this through the skin depth we find

$$\boxed{\int_0^\infty \overline{\mathbf{J} \times \mathbf{B}}\,dx = \frac{B_0^2}{4\mu}\hat{\mathbf{e}}_x} \tag{12.6}$$

This is the repulsion force anticipated in the previous section. Of course, $B_0^2/4\mu$ is simply the magnetic pressure which is an inevitable consequence of $|\mathbf{B}|$ dropping from B_0 to zero across the skin depth.

It is also of interest to calculate the Joule dissipation, J^2/σ, within the fluid. Integrating J^2/σ across the skin depth gives the net heating rate per unit surface area. It is readily confirmed that

$$\boxed{\dot{q} = \int_0^\infty (J^2/\sigma)\,dx = (B_0^2/4\mu)\omega\delta} \tag{12.7}$$

Let us now consider some of the consequences of allowing B_0 to vary slowly along the surface, as indicated in Figure 12.2. Let L be a typical geometric length scale, say $B_0/(\partial B_0/\partial z)$. We shall take $L \gg \delta$. (Recall that this is our working definition of 'high-frequency'.) When $L \gg \delta$, expressions (12.6) and (12.7) remain valid (to leading order in δ/L) provided that B_0 is interpreted as the local field strength. However, allowing B_0 to vary slowly within z introduces an additional effect: it induces motion in the fluid.

Consider the simplest case where $\mathbf{B}$ is two-dimensional: $(B_x, 0, B_z)$. The variation of B_z along the surface implies that B_x is non-zero, and in fact $\nabla \cdot \mathbf{B} = 0$ fixes the horizontal field as

$$B_x = \frac{\delta}{2}\frac{\partial B_0}{\partial z}[\cos(\omega t - x/\delta) + \sin(\omega t - x/\delta)]\exp(-x/\delta) \tag{12.8}$$

Since we have a small but finite horizontal field, the Lorentz force takes on a slightly different form. To find this force it is convenient to rewrite $\mathbf{J} \times \mathbf{B}$ as

$$\mu\mathbf{J} \times \mathbf{B} = -\nabla(B^2/2) + (\mathbf{B} \cdot \nabla)\mathbf{B}$$

We now throw out all terms of order $(\delta/L)^2$ and smaller. The result is

$$\mu\mathbf{J} \times \mathbf{B} = -\nabla(B_z^2/2) + \left[B_z\frac{\partial B_z}{\partial z} + B_x\frac{\partial B_z}{\partial x}\right]\hat{\mathbf{e}}_z$$

This can be further simplified. Noting that

$$\partial B_z/\partial x = (B_0/\delta)\exp(-x/\delta)[-\cos(\omega t - x/\delta) + \sin(\omega t - x/\delta)]$$

it is evident that $B_x(\partial B_z/\partial x)$ has zero time average, and so the mean Lorentz force is

$$\overline{\mathbf{J} \times \mathbf{B}} = -\nabla\left[\frac{B_0^2}{4\mu}\exp(-2x/\delta)\right] + \left[\frac{B_0}{2\mu}\frac{\partial B_0}{\partial z}\exp(-2x/\delta)\right]\hat{\mathbf{e}}_z \qquad (12.9)$$

We may regard $\overline{\mathbf{J} \times \mathbf{B}}$ as being composed of two parts. The first is irrotational and for confined fluids this merely supplements the fluid pressure. It is this term which leads to the magnetic pressure, $B_0^2/4\mu$. The second term is rotational and so cannot be balanced by the fluid pressure. It is much smaller than the first and is directed along the surface towards the peak value of B_0. This tangential force drives a fluid motion within the skin depth, pushing fluid from regions of low magnetic pressure to those of high magnetic pressure, as shown in Figure 12.4.

In summary, then, a high-frequency magnetic field, imposed at the boundary of a conducting fluid, has three effects:

(i) it repels the surface with a magnetic pressure of $B_0^2/4\mu$;
(ii) it generates heat at a rate of $(B_0^2/4\mu)\,\omega\delta$ per unit surface area;
(iii) it induces a tangential force $\partial/\partial z(B_0^2/4\mu)\exp(-2x/)\hat{\mathbf{e}}_z$ which drives fluid motion from regions of low magnetic pressure to regions of high pressure.

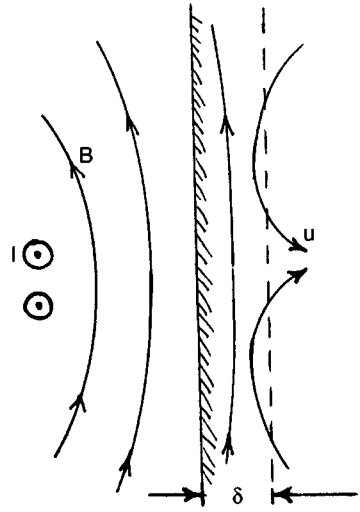

Figure 12.4 Motion induced by a variation in surface field strength.

12.3 Applications in the Casting of Steel, Aluminium and Super-Alloys

12.3.1 The induction furnace

The first induction furnace was designed by Ferranti in 1887. It reached more or less its present form around the turn of the century and has changed very little over the last one hundred years. The so-called 'coreless' induction furnace consists of a cylindrical, refractory vessel, filled with liquid metal, and surrounded by a high-frequency induction coil in the form of a solenoid. The coil generates a magnetic field which is almost parallel to the axis of the vessel, but which is confined to the skin depth of the molten pool. The primary purpose of the magnetic field is to heat the metal, although it has the added effect of stirring the liquid. This stirring turns out to be useful because it provides an effective mechanism for transporting the heat created at the boundaries into the interior of the liquid. However, it has the disadvantage that excessive velocities can lead to the erosion of the vessel wall.

We have already seen that the stirring force is confined to regions where the magnetic field varies along the surface of the melt. That is to say, the rotational component of $\overline{\mathbf{J} \times \mathbf{B}}$ is, from (12.9),

$$\mathbf{F}_r = \frac{\partial}{\partial s}\left(\frac{B_0^2}{4\mu}\right)\exp(-2n/\delta)\hat{\mathbf{e}}_s \tag{12.10}$$

Here the subscript 'r' indicates a rotational force, $B_0(s)$ is the surface field, s is a coordinate measured along the boundary and n is the distance from the surface. An inspection of Figure 12.5 suggests that this stirring force is confined largely to the corner regions of the furnace where the magnetic field enters and leaves the metal. In fact, this is often the case, and so the motion in the fluid is largely determined by the magnetic field distribution in a relatively small part of the furnace. This has two consequences. First, there exists the interesting possibility of controlling the flow by making small local changes to **B**. Second, if the driving force for **u** is rather sensitive to small geometrical features then it may be difficult to formulate simple, reliable estimates of $|\mathbf{u}|$. Still, we might expect the gross flow pattern to be like that shown in Figure 12.5. The rotational Lorentz force will drive fluid along the walls from the corner regions, where the magnetic pressure is low, to the midplane of the furnace where B_0 is high. This flow will then recirculate back through the core of the furnace, giving us an axisymmetric flow pattern consisting of two toroidal vortices. (If the stirring force in one

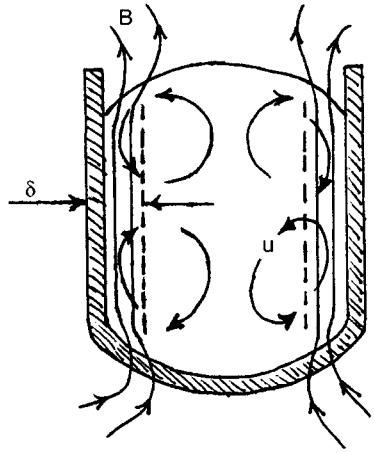

Figure 12.5 An induction furnace.

corner greatly outweighs the force in the other, then one of the toroidal vortices may be suppressed.

We shall now try to estimate the magnitude of $|\mathbf{u}|$. The procedure is somewhat circuitous, in that we first estimate the turbulence level in the furnace and then try to estimate the magnitude of the mean flow which would support such a level of turbulence. The arguments are all a bit rough and ready, but they do furnish estimates which are reasonably in line with experiments.

The starting point is to integrate the time-averaged Navier–Stokes equation around a closed streamline. When conditions are steady on average, this yields

$$\frac{1}{\rho}\oint \mathbf{F}_r \cdot d\mathbf{l} + \oint \frac{\partial}{\partial x_i}\left(\frac{\tau_{ij}}{\rho}\right) dl_j = 0 \tag{12.11}$$

where $\mathbf{u}$ is time-averaged velocity and τ_{ij} is the Reynolds stress. This represents an energy balance. It states that the work done by $\mathbf{F}_r$ on a fluid particle moving once around a closed streamline must be exactly balanced by the (negative) work done by the frictional shear stresses. If the two did not balance then the fluid particle would return to its starting position with a different mean energy, which cannot be the case in a steady-on-average flow. Now τ_{ij} might be estimated as $\tau_{ij} \sim \rho u'^2$ where u' is a measure of the fluctuating velocity. It follows from (12.11) that

$$\oint \mathbf{F}_r \cdot d\mathbf{l} \sim \rho u'^2 l / l_\tau$$

where l is a characteristic geometric length scale and l_τ is a typical length scale for cross-stream gradients in τ_{ij}. Substituting for $\mathbf{F}_r$ yields

$$u' \sim \frac{B_0}{\sqrt{\rho\mu}} \left(\frac{l_\tau}{l}\right)^{1/2}$$

However, we are interested in the mean velocity $\mathbf{u}$, rather than u'. In many forced, confined flows u' is around one-third of the peak mean velocity. If this is true in an induction furnace (and there are measurements to suggest it is), we might anticipate that the peak stirring velocity is of the order of

$$u \sim \frac{3B_0}{(\rho\mu)^{1/2}} \left(\frac{l_\tau}{l}\right)^{1/2} \tag{12.12}$$

The next question is, of course: what is l_τ? Some researchers assume that, since $\mathbf{F}_r$ is concentrated in a thin surface region of thickness δ, the flow near the wall must consist of thin wall jets, of thickness δ, which are driven by $\mathbf{F}_r$. These jets start near the corners of the furnace and direct fluid along the walls towards the mid-plane where opposing jets collide, driving fluid out into the core. If this is all true, then the bulk of the turbulent dissipation will be confined to the wall regions. In such cases l_τ should be taken as δ, and (12.12) yields (Hunt & Maxey, 1980)

$$u \sim \frac{3B_0}{(\rho\mu)^{1/2}} \left(\frac{\delta}{l}\right)^{1/2} \tag{12.13a}$$

An alternative possibility is that jets do not form and so the dissipation is distributed across the whole of the flow, in which case $l_\tau \sim l$ and we have the simpler estimate

$$u \sim \frac{3B_0}{(\rho\mu)^{1/2}} \tag{12.13b}$$

There are many assumptions and approximations built into (12.13a, b). Somewhat surprisingly, the experimental data tend to support (12.13a, b). It is found that u does indeed scale linearly with $B_0/(\rho\mu)^{1/2}$, and typically it is of the order of $B_0/(\rho\mu)^{1/2}$. It is less clear, however, which of these two estimates is the better. In most experiments $(\delta/l)^{1/2}$is around $0.4 \rightarrow 0.8$, and in view of the uncertainty in the multiplying factor of 3 it is not possible to distinguish clearly between (12.13a) and (12.13b) by simply examining the magnitude of u. A better test is to examine the dependence of u on ω, since (12.13a) suggests $u \sim \omega^{-1/4}$ while (12.13b) gives u independent of ω. The experiments indicate a behaviour some-

where between the two (Taberlet & Fautrelle, 1985), suggesting that (12.13a,b) are really too simplistic and that a more detailed analysis is required. So one hundred years after its introduction, we are still unable to estimate the velocity induced in an induction furnace!

12.3.2 The cold crucible

We now consider a device known as the cold crucible. This is designed to both melt and cast a metal in a single operation. The upper part of the crucible acts like an induction furnace, into which solid material is fed. This is inductively melted to form a liquid pool. The lower part acts like a casting mould, in which the liquid metal freezes on contact with the cold walls of the crucible. In steady-state operation solid fragments are continually fed in from above, while an ingot is withdrawn from the bottom. A schematic representation of the process is shown in Figure 12.6.

The name 'cold crucible' derives from the fact that the walls of the vessel are constructed from water-cooled metal segments which cause the molten pool to freeze on contact with the vessel wall. This is quite different from an induction furnace whose insulating, refractory walls are hot, leaving the metal as a liquid. The ingenious part of the cold crucible lies in the construction of the wall. In order to heat the metal it is necessary to find some way of allowing the magnetic field to pass through the conducting wall of the crucible. This is achieved by segmenting the wall, as shown in Figure 12.6. Each segment is electrically insulated and so the eddy currents which are induced in the outer surface of the wall, and which would ordinarily shield the interior from the applied field, are forced to recirculate around each segment. The end result is a smooth distribution of current on the inside surface of the wall, which in turn generates a magnetic field in the interior of the crucible. It is as if the segmented wall is transparent to the magnetic field. The lower part of the vessel acts just like a conventional casting mould, with the liquid freezing on contact with the water-cooled metal wall. As in conventional casting, it is necessary to feed small quantities of casting flux down the gap between the ingot and the crucible wall. This acts as a lubricant and provides a thin thermal barrier between the ingot and the walls.

Cold crucibles are also used to melt material in batches, rather like an induction furnace. In such cases the bottom of the crucible is blanked off using a segmented, water-cooled plate. The bulk of the crucible contents is then liquid, but we retain a thin crust of solid metal (called a skull)

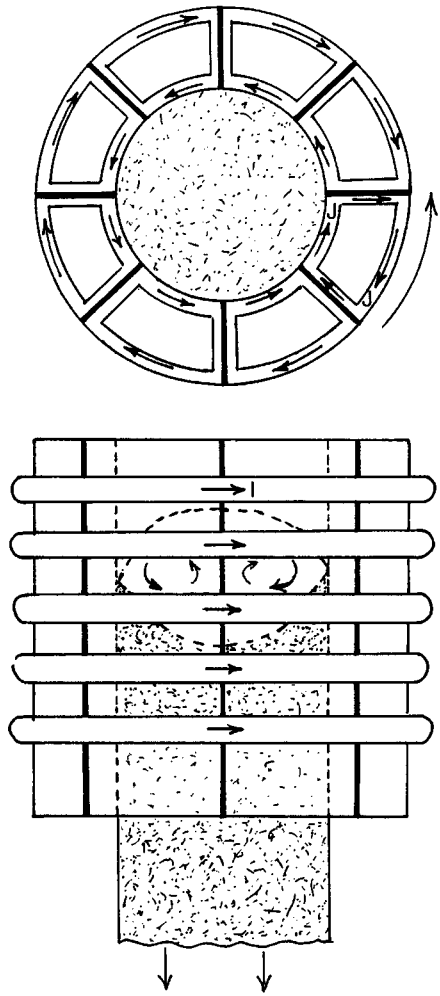

Figure 12.6 A cold crucible consists of water-cooled segments surrounded by a high-frequency induction coil.

adjacent to the walls and base. This is often used to melt highly reactive metals, such as titanium or nickel, which would attack the refractory walls of a conventional furnace.

12.3.3 Levitation melting

We now turn to industrial and laboratory processes where the primary function of the magnetic field is to levitate or repel the liquid metal.

These, of course, rely on the existence of the magnetic pressure, $B_0^2/4\mu$. In this section we focus on levitation melting, a technique which was first suggested in 1923, but had to wait until the 1950s to be tried in the laboratory, and the 1960s to be developed commercially.

Levitation melting is now commonly used in the laboratory as a means of melting small specimens of highly reactive metal. It is also used as a means of measuring the surface tension of liquid metals. The topics we will discuss here are:

(i) the shape of the levitation coils;
(ii) the fact that the process is pseudo-static (the induced velocities are low);
(iii) there is a limit on the drop size which may be levitated;
(iv) a method for calculating the drop shape;
(v) a variational principle associated with the drop shape.

A simple levitation device is shown in Figure 12.7. It consists of a lower toroidal coil, wound into a basket shape, above which sits the metal droplet. A second, smaller, coil is located above the specimen and this carries a current which is 180° out of phase with the lower coil. We shall see shortly that there is a strict limit to the size of specimens which may be levitated in this way: typically the droplet size is no more than one or two centimetres. Since we require $\delta \ll$ (drop size) in order to generate magnetic pressure, this implies that high frequencies are required, of the order of 100 kHz.

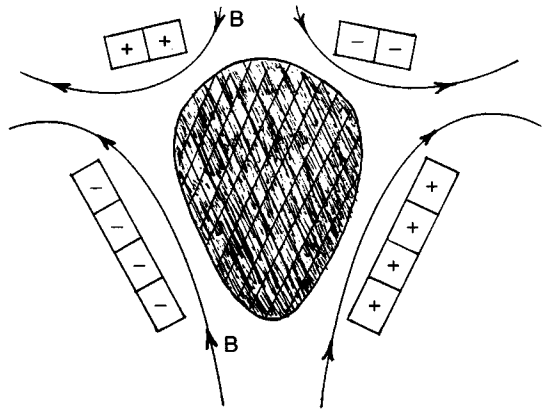

Figure 12.7 Levitation melting of a small metal specimen.

The two coils shown in Figure 12.7 have rather different functions. The lower coil provides support against the weight of the metal. The top coil, on the other hand, is required to provide stability. That is, the introduction of the upper coil creates a field configuration which, in the absence of the specimen, has a null point somewhere on the axis between the two coils. A small test specimen placed at such a point is stable to small lateral movements because any movement of the specimen brings it into a region of higher magnetic field, and the resulting change in magnetic pressure will tend to push the metal back towards the null point. At least that is the theory. In practice, instabilities such as vertical oscillations and rotations often develop.

In order to understand the shape of the levitated droplet, and to predict the maximum mass which can be levitated, it is necessary to consider the balance between magnetic pressure, fluid pressure (which is due to self-weight) and surface tension. Usually this balance may be treated as pseudo-static, in the sense that the effect of motion on the fluid pressure may be ignored. The reason for this simplification is as follows. The rotational component of the Lorentz force, which drives motion in the droplet, is of order $|\mathbf{F}_r| \sim B_0^2/\mu l$ where B_0 is the surface field strength and l is a typical geometric length scale (say the droplet size). This force acts parallel to the surface. Now suppose we integrate this through the (narrow) skin depth and replace the distributed force by an effective shear stress of order $\tau \sim (B_0^2/\mu)(\delta/l)$. Compare this with the magnetic pressure, $p_m = B_0^2/4\mu$. Evidently, since δ is much less than l, we have $\tau \sim p_m(\delta/l) \ll p_m$. However, τ leads to fluid motion, while p_m counterbalances the hydrostatic pressure, and so we would expect $\rho u^2 \ll \rho g l$ in the limit of $\delta \ll l$. Thus, if our sole purpose is to determine the equilibrium shape of the drop, we may ignore $\mathbf{F}_r$ and the associated motion within the liquid. It follows that the surface shape is determined by the pseudo-static force balance

$$\frac{B_0^2}{4\mu} + \rho g z + \gamma K = \text{constant}$$

where K is the surface curvature, z is the vertical position of the surface and γ is the surface tension coefficient. If we take the origin of z to be at the base of the droplet, and note that the Lorentz force is zero at $z = 0$, we obtain

$$\frac{B_0^2}{4\mu} + \rho g z + \gamma K = \gamma K_0 \tag{12.14}$$

where K_0 is the curvature at the base of the drop.

It is now clear that there is a fundamental limitation to this process. In any axisymmetric configuration the induced currents fall to zero on the axis, and so the magnetic pressure is zero at the base and the top of the drop. It follows that the hydrostatic pressure on the axis must be balanced by surface tension alone, and this limits the height of the droplet which can be levitated. We can estimate this critical height, h_c, from (12.14). The maximum value of K_0 will be of order δ^{-1}, since we require the local droplet thickness to be greater than δ in order to maintain some magnetic pressure. If we take K at the top of the drop to be much less than K_0, which seems reasonable, then (12.14) gives $\rho g h_c \sim \gamma/\delta$ and so the critical height is of the order of

$$h_c \sim \gamma/\rho g \delta \tag{12.15}$$

Drops larger than this will tend to drip near the axis.

The process of calculating the drop shape, although pseudo-static, is still non-trivial. This is because the shape depends on the distribution of $\mathbf{B}_0(s)$, the surface field strength. Yet $\mathbf{B}_0(s)$ itself depends on the presence and shape of the drop since the field is excluded from the interior of the drop and so must deform around its surface. In general, it is necessary to adopt an iterative approach to calculate the shape, in which an initial guess of the surface profile leads to a provisional estimate of $\mathbf{B}_0(s)$. (This is obtained by solving $\nabla \cdot \mathbf{B} = 0$ and $\nabla \times \mathbf{B} = 0$ outside the droplet, subject to $\mathbf{B} \cdot \mathbf{n} = 0$ on the drop surface.) From this estimate of $\mathbf{B}_0(s)$ the magnetic pressure can be calculated and compared with that required to hold the droplet in its chosen shape. At points the actual magnetic pressure will be greater than that required by (12.14) and at other positions it will be too small. The surface shape is then changed slightly, moving outward at places where p_m is found to be too small and inward where p_m is excessive. The procedure is now repeated for the new estimate of the drop shape. After a few iterations a solution of (12.14) can be found which is compatible with the external coil geometry.

An alternative iterative procedure for calculating the drop shape can be established using a variational principle. This principle applies only in the limit $\delta \to 0$ and assumes that the electric current in the external coils is fixed and independent of the droplet shape. We proceed as follows. We know that the equilibrium configuration, if stable, must correspond to a minimum value of $E_g + E_\gamma + E_p$ where E_g is the total gravitational potential energy, E_γ is the surface tension energy, and E_p is the potential energy associated with the magnetic pressure. This latter energy is the work done

against p_m by the fluid boundary in establishing the presence of the drop. (Imagine blowing up a balloon which is subject to some external pressure.) The complication is that p_m itself depends on the presence and shape of the drop, and so we need some way of calculating E_p. It turns out that, to within a constant, E_p is (minus) the energy of the external magnetic field.

To see why this is so, consider what happens if the surface S of the droplet deforms slightly. Let δn be the movement of the surface at any point on S, being positive if outward and negative if inward. We now deform the drop, while conserving volume. The work done by the fluid against p_m is

$$\delta W = \oint_S p_m \delta n dS$$

It follows that the increase in E_p caused by this movement is

$$\delta E_p = \oint_S (B_0^2/4\mu)\delta n dS \tag{12.16}$$

Now consider the change in magnetic energy E_B associated with the deformation of the surface. This comes in two parts. First there is the reduction in E_B associated with the fact that the small volume $\delta n dS$ previously contained a magnetic field which had an energy of $(B_0^2/4\mu)(\delta n dS)$. Second, the deformation of the drop changes the eddy currents circulating in its surface, and this leads to a change in the external magnetic field. If V_{ext} is external volume we have

$$\delta E_B = \delta \int_{V_{ext}} (B^2/4\mu) dV - \oint_S (B_0^2/4\mu)\delta n dS \tag{12.17}$$

However, it is easily seen that the first integral is zero. To this end we write $\mathbf{B} = \mathbf{B}_1 + \mathbf{B}_2$, where $\mathbf{B}_1$ is the field due to the coil which would exist in the absence of the drop and $\mathbf{B}_2$ is the field associated with the eddy currents in the surface S. Within the drop $\mathbf{B}_1$ and $\mathbf{B}_2$ are equal and opposite. Outside we have $\delta(\mathbf{B}^2) = 2\mathbf{B} \cdot \delta\mathbf{B} = 2\mathbf{B} \cdot \delta\mathbf{B}_2$ since $\delta\mathbf{B}_1 = 0$, the coil current being fixed. However, $\delta\mathbf{B}_2$ satisfies $\nabla \times \mathbf{B} = 0$ in V_{ext} and so this can be written as $\delta\mathbf{B}_2 = \nabla(\phi)$. This yields $\delta(\mathbf{B}^2) = 2\nabla \cdot (\phi\mathbf{B})$, which integrates to zero in V_{ext} since $\mathbf{B} \to 0$ at infinity and $\mathbf{B} \cdot \mathbf{n} = 0$ on S. It follows that

$$\delta E_B = -\oint_S (B_0^2/4\mu)\delta n dS = -\delta E_p \tag{12.18}$$

It follows that the equilibrium configuration corresponds to a stationary value of $E_g + E_\gamma - E_B$ (Sneyd & Moffatt, 1982). This provides the basis for an alternative iterative procedure for finding the droplet shape, i.e. the boundary is systematically deformed so as to minimise $E_g + E_\gamma - E_B$.

12.3.4 Processes which rely on magnetic repulsion: EM valves and EM casters

Suppose we increase the mass of the droplet shown in Figure 12.7 until the critical height, h_c, is exceeded. The drop will start to drip, and if h is made large enough a small jet will emerge, centred on the axis. If the droplet mass is continually replenished from above we have a rudimentary form of electromagnetic valve. The simplest embodiment of such a device is shown in Figure 12.8. This provides a means of modulating the flow of a liquid-metal jet without the need for any moving mechanical part. By increasing the power in the induction coil, the flow rate through the electromagnetic valve is reduced.

A simple estimate of the reduction in flow rate may be determined by applying Bernoulli's equation from some upstream location, say the surface of the reservoir which feeds the valve, to the point at which the jet separates from the nozzle wall. The pressure in the jet at the separation point is p_m (atmospheric pressure being taken as a datum for pressure). In the absence of friction, Bernoulli's equation yields

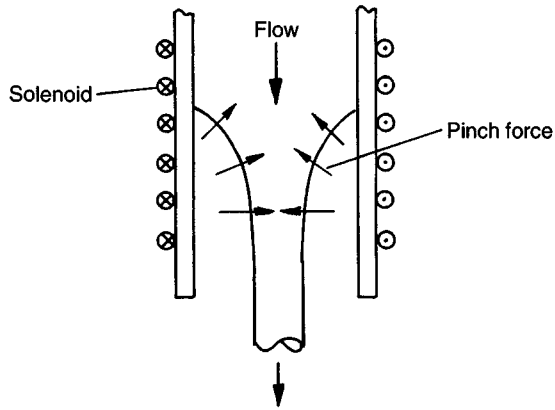

Figure 12.8 A simple electromagnetic valve.

$$\rho g H = \frac{1}{2}\rho u^2 + p_m$$

where H is the head of liquid above the separation point. The mean velocity at the separation point is then

$$u = \left[2gH - B_0^2/(2\rho\mu)\right]^{1/2} \tag{12.19}$$

Of course, this is a rather simplistic estimate, which ignores frictional losses and variations in velocity across the jet. For example, it predicts that the flow is completely shut off at a critical value of magnetic pressure, $p_m = \rho g H$, yet we have already seen that this cannot be true in an axisymmetric configuration. Nevertheless, experiments suggest that (12.19) captures the gross behaviour of the device provided p_m is not too close to the critical value.

A quite different application of magnetic repulsion is illustrated in Figure 12.9. This shows the electromagnetic casting of aluminium, a process which was developed by Getselev in the USSR in 1971 and is now used throughout Europe and North America. In effect, it is identical to the conventional casting of aluminium except that the water-cooled mould which normally surrounds the liquid pool (see Figure 8.1) is replaced by a high-frequency induction coil. However, the mould and coil fulfil similar rôles: they are both required to maintain the pool shape, the former achieving this by mechanical support while the latter uses magnetic pressure. Remarkably, the process turns out to be stable. The primary advantage of electromagnetic casting is that the surface quality of the ingot is improved. This means that the ingot surface does not require machining prior to rolling.

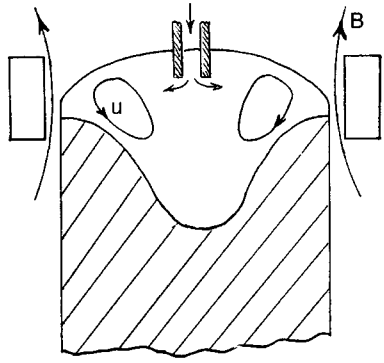

Figure 12.9 Electromagnetic casting of aluminium.